A Comparative Study of SILC Transient Characteristics and Mechanisms in FN Stressed and Hot Hole Stressed Tunnel Oxides

Nian-Kai Zous, Tahui Wang, Chih-Chich Yeh, Ching-Wei Tsai, and Chimoon Huang*

Department of Electronics Engineering, National Chiao-Tung University
*Winbond Electronics Corp.
Hsin-Chu, Taiwan, R.O.C.
fax:886-3-5724361;email:wang@jekyll.ee.nctu.edu.tw

Abstract

The mechanisms and transient characteristics of hot hole stress and FN stress induced excess leakage currents in tunnel oxides are investigated. Hot hole SILC is found to have a more pronounced transient effect. The transient is attributed to positive oxide charge detrapping and thus annihilation of positive charge-assisted tunneling current. The positive charge assisted tunneling current can be annealed by substrate hot electron injection. The DC and transient components in FN SILC are also discussed.

Introduction

High field stressing during program/erase cycles in flash EEPROM operation can lead to a significant increase in low-level leakage current in tunnel oxides. Stress induced leakage current (SILC) has received a lot of attention recently because of its important significance to the data retention and endurance characteristics of a flash memory cell [1-10]. Several mechanisms were proposed for SILC including positive charge-assisted tunneling (PCAT) [1], neutral trap-assisted tunneling [2] and thermally-assisted tunneling at weak spots of the Si/SiO_2 surface due to a barrier height lowering [3]. Despite extensive studies on SILC, its physical mechanism still remains controversial. DiMaria et al concluded from their experimental result [8] that positive oxide charge plays no part in the SILC conduction mechanism in oxides by FN stress. Contrarily, Teramoto et al claimed that the excess leakage current induced by FN stress is caused by the injected holes produced by high energy electrons [9]. Shuto et al have further shown that hot hole (HH) injection during source-side FN erase is the major cause of read-disturb degradation in flash devices [10].

In addition, Dumin et al found that FN stress induced leakage current contains a transient component and a DC component [5]. In their work, the transient current is attributed to oxide trap charging and discharging and the DC component is via neutral trap assisted tunneling. The former can be characterized by a $1/t$ time-dependence from the tunneling front model. A threshold voltage shift of 1.0V resulting from a SILC transient component was reported by Kato et al [6]. Although tremendous efforts have been made to investigate the SILC transient effects and mechanisms, most of previous research was concentrated on SILC by channel FN stress. In this work, we intend to explore the SILC transient behavior by HH stress. The role of positive oxide charge in FN SILC and HH SILC will be investigated.

To measure FN and HH SILCs directly, a n-MOSFET with a long drain edge was specially fabricated. The test device has a gate length of 0.6μm and a total gate area of $9x10^{-4}cm^2$. The oxide thickness (t_{ox}) is about 10nm. The measured FN SILC and HH SILC are shown in Fig. 1. The channel FN stress is at V_{gs}=-11V for 3000 second and the drain avalanche HH stress is performed at V_{gs}=-0.5V and V_{ds}=7V for 300 seconds. The created oxide trapped charge Q_{ox} in the two stressed devices is monitored by using a threshold voltage method and a GIDL current method [11] respectively. The reason of measuring GIDL shift for the HH stressed device is that threshold voltage in a n-MOSFET is not sensitive to localized positive oxide charge. Fig. 2 shows the Id-V_{gs} curves before and after HH stress. After the stress, GIDL current shifts to the left and threshold voltage is nearly unchanged. In Fig. 1, the HH SILC appears to have a more pronounced transient effect. Its transient current is about an order of magnitude larger than that of the FN SILC. The shaded areas denoted by Q_g(FN) and Q_g(HH) represent an integral of the SILC transients in a measurement period from 0.1 second to 300 seconds. In other words, Q_g(FN) and Q_g(HH) are total charge flowing to the gate carried by the transient component of the SILC's. The measured Q_{ox} and Q_g in the two devices are compared in Table 1 [12]. It is interesting to note that Q_g(FN) is less than Q_{ox}(FN) while Q_g(HH) is about twenty times larger than Q_{ox}(HH). The result Q_g(FN)<Q_{ox}(FN) is understood because the FN SILC transient is caused by oxide charge detrapping. Thus, Q_g(FN) should not exceed the total charge stored in the oxide. On the other side, the result Q_g(HH)>>Q_{ox}(HH) implies that the HH SILC should contain another leakage component in addition to oxide charge trapping/detrapping. Our statement is also supported by the work of Teramoto [9].

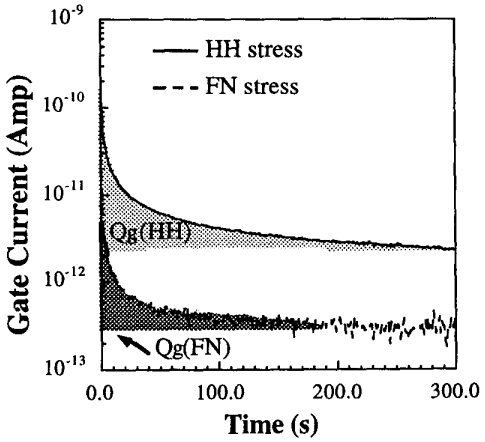

Fig. 1 HH stress and FN stress induced leakage current transients at a measurement field of 6MV/cm. The shaded areas Q_g(FN) and Q_g(HH) represent total charge flowing to the gate carried by the transient component of the SILC's in the measurement period.

0-7803-5220-3/99/$10.00 ©1999 IEEE

IEEE 99CH36296. 37th Annual International Reliability Physics Symposium, San Diego, California, 1999

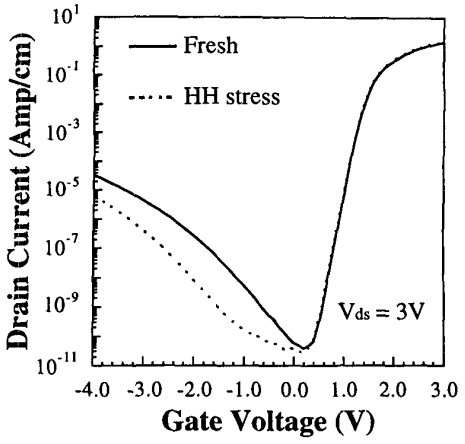

Fig. 2 Normalized I_d-V_{gs} curves before and after HH stress. After stress, GIDL current shifts to the left and V_{th} is unchanged.

Moreover, we plot the FN and HH SILC transients on a *log-log* scale in Fig. 3. Both the transients follow a straight line, or a power law time-dependence. However, a slight difference in the slope of the two transients is observed. The FN SILC has a slope about -0.9. The HH SILC in Fig. 3 was measured carefully and for three decades of time. The slope significantly deviates from the theoretical value of -1 [5]. The difference in the two slopes gives an evidence that the FN SILC and HH SILC should have a different transient mechanism.

Table 1 Measured Q_g and Q_{ox} in HH stressed and FN stressed n-MOSFET's. Q_g is normalized to a total stressed gate area. The width of the HH stress region in the channel is assumed to be 0.2μm. e denotes an elementary charge ($1.6x10^{-19}$C).

	Q_g (e/cm^2)	Q_{ox} (e/cm^2)	$\lvert Q_g / Q_{ox} \rvert$
HH	$2.7x10^{13}$	$1.2x10^{12}$	22.5
FN	$4.6x10^{11}$	$-1.5x10^{12}$	0.31

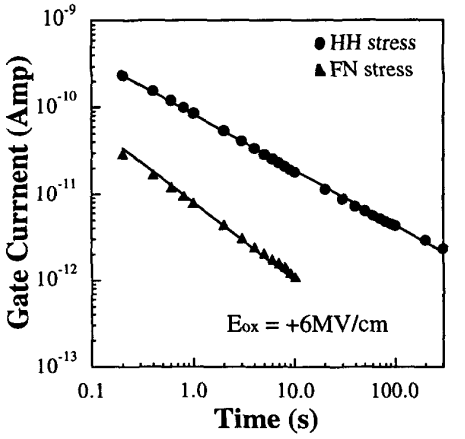

Fig. 3 FN and HH SILC transients are plotted on a *log(I)-log(t)* scale.

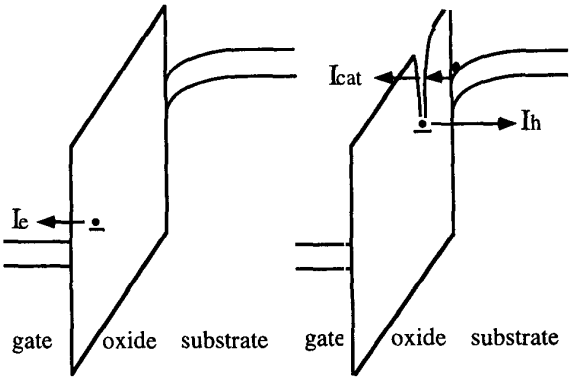

(a) (b)

Fig. 4 Illustration of SILC transient mechanisms at a positive measurement field. (a) a F/N stressed device and (b) a HH stressed device.

HH Stress Induced Leakage Current

Fig. 4 illustrates the SILC transient mechanisms in the two stressed devices. In the FN stressed device (Fig.4(a)), the SILC transient is assumed to be dominated by negative oxide charge detrapping. Here, we would like to remark that positive oxide charge creation, in fact, is expected during FN stress. However, the role of positive oxide charge in FN SILC is not certain, depending on factors such as oxide thickness, stress time, stress field and measurement polarity [13]. The HH SILC transient consists of two major components (Fig. 4(b)). One is positive oxide charge detrapping current (I_h) and the other is positive oxide charge assisted electron tunneling current (I_{cat}). For Q_g(HH)>>Q_{ox}(HH), the HH SILC is dictated by I_{cat}. The transient behavior of I_{cat} arises from that the positive oxide charges, which help electrons to tunnel through the oxide, can themselves escape to the Si substrate via tunneling in measurement. An analytical model relating the time-dependence of I_{cat} to positive oxide charge tunnel detrapping is derived in [12]. It can be shown that both I_{cat} and I_h obey a power law time-dependence as follows,

$$I_{cat} \propto q \frac{\overline{N_h}}{\tau_{oe}\alpha_h}\left(\frac{\tau_{oh}}{t}\right)^p \Gamma(p), \quad (1)$$

$$p = \left(\frac{m_e(q\phi_0)}{m_h E_t}\right)^{1/2} \quad (2)$$

where $\alpha_h = 4\pi(2m_h E_t)^{1/2}/h$, $\overline{N_h}$ represents an average oxide charge volumetric concentration, Γ in Eq. (1) denotes the Gamma function, τ_{oe} and τ_{oh} are electron and hole tunneling characteristic times [14], $q\phi_0$ and E_t are effective tunneling barrier heights for electrons and holes respectively, and other variables have their usual definitions. Similarly, the expression for I_h is given below,

$$I_h = Aq\frac{\overline{N_h}}{\alpha_h}t^{-1} \quad (3)$$

where A is the area of the HH stress region.

The extracted slope of the HH SILC in Fig. 3 is about -0.7. Although it is difficult to compare our model with the measured result directly due to uncertainties in the parameters in Eq. (2), it is a general trend in literature to have $m_h \geq m_e$ [15,18,19] and $E_t \geq q\phi_0$ [17,16]. Thus, the power factor p in Eq. (2) should be smaller than 1, which is in agreement with the measurement result.

Note that I_{cat} is an electron tunneling current, which flows from the gate to the source or the drain at a positive measurement gate bias. As a contrast, I_h is a hole tunneling current, flowing to the substrate. In Fig. 5, we draw I_g and I_{sub} (substrate current) before and after HH stress. The pre-stress I_{sub} is negligible until V_{gs} is above 8V, where the origins of I_{sub} have been identified [20]. After HH stress, a remarkable I_{sub} exists even at a small gate bias. The appearance of I_{sub} results from the discharging of the stress created hole traps near the substrate and provides a direct evidence that positive oxide charge plays an important role in the HH SILC.

The field-dependence of the HH SILC transient is investigated in Fig. 6. The gate bias increases from 4.3V to 6.3V with an increment of 0.5V each line. From the results in Figs. 5 and 6, the HH SILC shows a relatively weak field dependence in the low field region (V_{gs}<5V) and has a stronger field dependence in the medium field region.

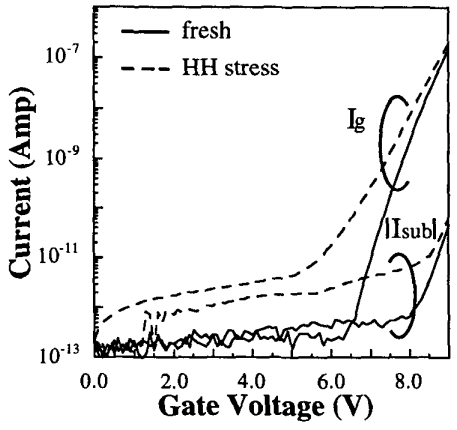

Fig. 5 Gate current and substrate current versus measurement gate bias before and after HH stress.

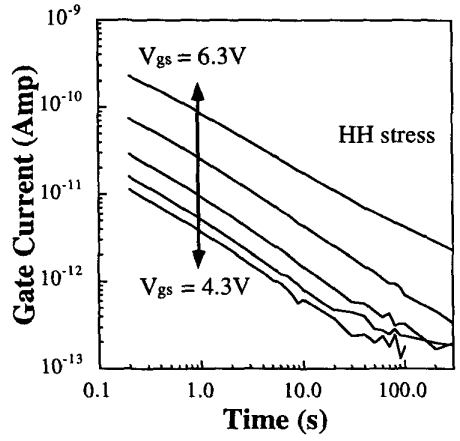

Fig. 6 Dependence of a HH SILC transient on measurement gate bias. V_{gs} increases from 4.3V to 6.3V with an increment of 0.5V each line.

FN Stress Induced Leakage Current

In Fig. 7, the time-dependence of FN SILC at different stress times is shown. The stress bias is V_{gs}=+9.5V. The measurement oxide field is about +6MV/cm, the same as in Fig. 1. The oxide field is estimated from $(V_g-V_{fb})/t_{ox}$, where V_{fb} is the flat-band voltage. As compared to the -FN SILC in Fig. 3, the +FN SILC apparently has a larger DC component while its transient component is smaller. In Fig. 8, we replot the +FN transient component and the DC component versus stress time separately. The transient current is obtained from the total current measured at t=0.2 seconds subtracted by the steady-state current. While the transient component increases monotonically with stress time, the DC component shows a turn-around feature; i.e. the DC current first increases with stress time and then decreases with it. The corresponding stressing gate current versus stress time is shown in Fig. 9.

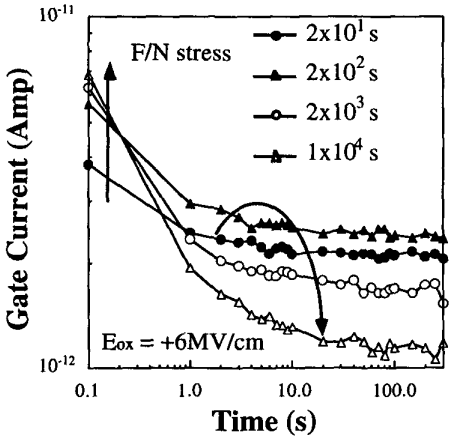

Fig. 7 FN SILC measured at stress times of $2x10^1$ sec., $2x10^2$ sec., $2x10^3$ sec., and $1x10^4$ sec.

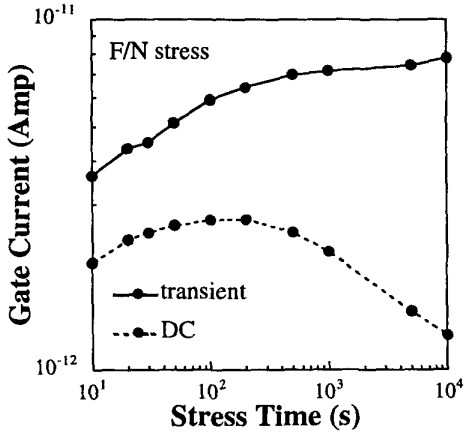

Fig. 8 Evolution of DC and transient components of a +FN SILC with stress time.

A strong similarity in the stress time dependence in Figs. 8 and 9 is obtained. The turn-around characteristic of the FN stress gate current has been realized due to positive oxide charge creation in an early stage of stress. Thus, we strongly believe that the DC component of the +FN SILC is contributed, to some

extent, by the PCAT current. A similar turn-around feature in SILC was also reported by Moazzami [21].

Positive Oxide Charge Annealing

Another evidence for the existence of PCAT in the +FN SILC is that the DC component can be significantly reduced by annealing the positive oxide charges. Here, substrate hot electron (SHE) injection at V_{gs}=2.5V and V_{sub}=-7V is utilized

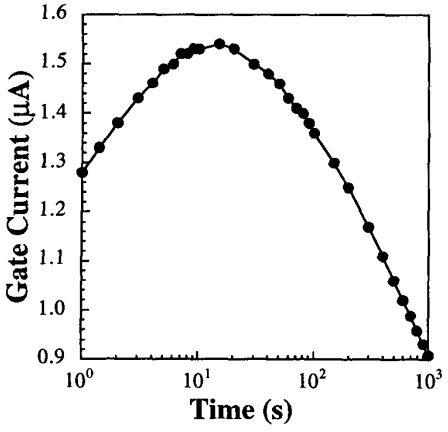

Fig.9 Stressing gate current versus stress time under constant voltage stress at V_{gs} = 9.5V. Hole-trap generation is dominant at an early stage of stress.

to neutralize the PCAT centers. Since the substrate injection current is relatively large ($2x10^{-4}A/cm^2$), positive oxide charge neutralization is achieved via recombination or compensation by the injected electrons. The substrate filling effect on the +FN SILC is shown in Fig. 10. After the filling, the transient component of the SILC increases because more electrons are stored in the oxide. On the contrary, the DC component declines for the reduction of the PCAT centers. It should be mentioned that the oxide leakage current after the filling is still above the current level in a fresh device. The excess leakage current is possibly due to neutral trap assisted tunneling. Also shown in Fig. 10 is a +FN SILC in a 4nm oxide. No transient effect in SILC [21] is observed and the SHE filling effect is negligible.

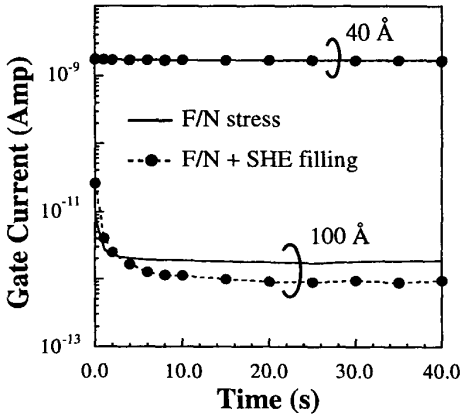

Fig. 10 SHE filling effect on +FN SILCs in a 10nm oxide and in a 4nm oxide.

The SHE filling effect on the HH SILC is shown in Fig. 11. The HH SILC is greatly reduced by the filling. Its steady-state level is below 1pA after the filling. After subsequent HH stress, the large transient reappears. The HH stress/SHE filling cycle repeats two times. No noticeable difference is observed between the two cycles, which suggests that the SHE filling itself does not introduce additional stress effects.

Conclusion

In a relatively thick oxide (10nm), no matter by FN stress or HH stress, the SILC is dominated by a transient component. The FN and HH SILC transients are found to have a different time-dependence. The responsible mechanisms are identified. Our study shows that PCAT is a dominant mechanism in a HH SILC and in the DC component of a +FN SILC. In an ultra-thin oxide (4nm), the SILC mechanism is trap-assisted tunneling and no appreciable transient effect is observed. By using a positive oxide charge neutralization technique, the PCAT current can be greatly reduced.

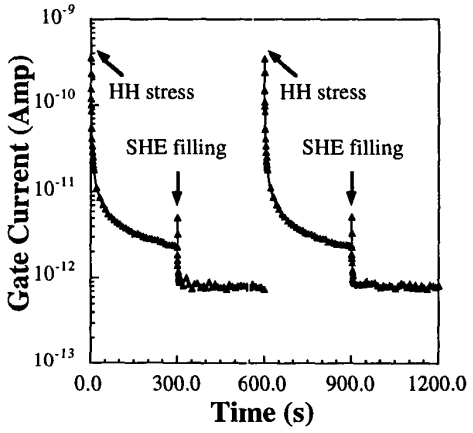

Fig. 11 SHE filling effect on HH SILC. t_{ox} = 10nm.

Acknowledgement

Financial support from National Science Council, ROC, under contract no. NSC88-2215-E009-042 is gratefully acknowledged.

References

[1] J. Maserjian and N. Zamani, "Observation of Positively Charged State Generation near the Si/SiO_2 Interface during Fowler-Nordheim Tunneling," *J. Vac. Sci. Tech.*, Vol. 20, pp. 743-746, 1982

[2] R. Rofan and C. Hu, "Stress-Induced Oxide Leakage," *IEEE Elect. Dev. Lett.*, Vol. 12, pp. 632-634, 1991

[3] P. Olivio, T. Nguyen and B. Ricco, "High Field Induced Degradation in Ultra-Thin SiO_2 Films," *IEEE Trans. Elect. Dev.*, Vol. 35, pp. 2259-2265, 1988

[4] N. Matsukawa, S. Yamada, K. Amemiya and H. Hazama, "A Hot Hole-Induced Low-Level Leakage Current in thin Silicon Dioxide Films," *IEEE Trans. Elect. Dev.*, Vol. 43, pp. 1924-1929, 1996

[5] D.J. Dumin and J. Maddux, "Correlation of Stress-Induced Leakage Current in Thin Oxides with Trap Generation Inside the Oxides." *IEEE Trans. Elect. Dev.*, Vol. 40, pp.

986-993, 1993

[6] M. Kato, N. Miyamoto, H. Kume, A. Satoh, M. Ushiyama and K. Kimura, "Read-Disturb Degradation Mechanism due to Electron Trapping in the Tunnel Oxide for Low-Voltage Flash Memories," *IEDM Tech. Dig.*, pp. 45-48, 1994

[7] E. Rosenbaum and L.F. Register, "Mechanism of Stress-Induced Leakage Current in MOS Capacitors," *IEEE Trans. Elect. Dev.*, Vol. 44, pp. 317-323, 1997

[8] D.J. DiMaria and E. Cartier, "Mechanism for Stress Induced Leakage Current in Thin SiO_2 Films," *J. Appl. Phys.*, Vol.78, pp. 3883-3894, 1995

[9] A. Teramoto, K. Kobayashi, Y. Matsui, M. Hirayama and K. Yasuoka, "Excess Currents Induced by Hot Hole Injection and FN Stress in Thin SiO_2 Film," *Proc. Int. Reliability Phys. Symp.*, pp. 113-116, 1996

[10] S. Shuto, S. Yamada, S. Aritome, T. Watanabe, K. Hashimito, "Read Disturb Degradation Mechanism for Source Erase Flash Memories," *Digest of Symp. on VLSI Tech.*, pp. 242-243, 1996

[11] T. Wang, T.E. Chang, L.P. Chiang, N.K. Zous and C. Huang, "Investigation of Oxide Charge Trapping and Detrapping in a n-MOSFET by Using a GIDL Current Technique," *IEEE Trans. Elect. Dev.*, Vol. 45, pp.1511-1517, 1998

[12] T. Wang, N.K. Zous, J.L. Lai and C. Huang, "Hot Hole Stress Induced Leakage Current Transient in Tunnel Oxides," *IEEE Elect. Dev. Lett.*, Vol. 19, pp. 411-413, 1998.

[13] A. Meinertzhagen, C. Petit, M. Joudain, F. Mondon, "Stress Induced Leakage Current Reduction by a Low field of Opposite Polarity to the Stress Field," *J. Appl. Phys.*, Vol.84, pp. 5070-5079, 1998

[14] I. Lundsorm and C. Svensson, "Tunneling to Traps in Insulator," *J. Appl. Phys.*, Vol. 43, pp. 5045-5047, 1972

[15] S. Manzini and A. Modelli, "Tunneling Discharge of Trapped Holes in Silicon Dioxide," in *Insulating Films on Semiconductors* edited by J. F. Verweij and Wolters, Elsevier Science Publishers, North Holland, pp. 112-115, 1983

[16] T.R. Oldham, A. J. Lelis and F.B. Mclean, "Spatial Dependence of Trapped Holes Determined from Tunneling Analysis and Measured Annealing," *IEEE Trans. Nucl. Sci.*, Vol. NS-33, pp. 1203-1209, 1986

[17] F.J. Grunthaner, B.F. Lewis, N. Zamini and J. Maserjian, "XPS Studies of Structure-Induced Radiation Effects at the Si/SiO_2 Interface," *IEEE Trans. Nucl. Sci.*, Vol. NS-27, pp. 1640-1646, 1980

[18] J.R. Chelikowsky and M. Schluter, "Electron States in α-Quartz: A Self-Consistent Pseudopotential Calculation," *Phys. Rev. B.*, Vol. 15, pp. 4020-4029, 1977

[19] B.Brar, G.D. Wilk and A.C. Seabaugh, "Direct Extraction of the Electron Tunneling Effective Mass in Ultrathin SiO_2," *Appl. Phys. Lett.*, Vol. 69, pp. 2728-2730, 1996

[20] I.C. Chen, S. Holland, K.K. Young, C. Chang and C. Hu, "Substrate Hole Current and Oxide Breakdown," *Appl. Phys. Lett.*, Vol. 49, pp. 669-671, 1986

[21] R. Moazzami and C. Hu, "Stress Induced Current in Thin Silicon Dioxide Films," *IEDM Tech. Dig.*, pp.139-142, 1992